

## RESEARCH ARTICLE

# Experimental demonstration and analysis of underwater wireless optical communication link: Design, BCH coded receiver diversity over the turbid and turbulent seawater channels

Prasad Naik Ramavath  |

Shripathi Acharya Udupi |

Prabu Krishnan 

Department of Electronics and Communication Engineering, National Institute of Technology Karnataka, Surathkal, Mangalore, Karnataka, India

## Correspondence

Prasad Naik Ramavath, Department of Electronics and Communication Engineering, National Institute of Technology Karnataka, Surathkal, Mangalore 575025, Karnataka, India.

Email: prasadnaikr@gmail.com

## Abstract

In this article, we demonstrate an experimental underwater wireless optical communication (UWOC) system in the presence of air bubbles and weak turbulence for varying turbidity levels of the aquatic optical medium. The major limiting factors of the UWOC system are: absorption, scattering, and beam fluctuations; these effects can be mitigated by employing transmitter/receiver diversity schemes and channel codes. In this proposed system, we have employed receiver diversity (selection combining (SC), majority logic combining (MLC), and equal gain combining (EGC)) techniques augmented with Bose-Chaudhuri-Hocquenghem (BCH) codes to improve the performance of on-off keying modulated UWOC system. The bit error rate (BER) expressions are derived for the proposed system and results are validated using analytic and experimental means. The results show that the proposed system, that is, the receiver employing SC, MLC, and EGC receiver combining techniques augmented with the BCH code provides a transmit power gain of 4, 6, and 8 dB respectively, when compared with the uncoded single-input single-output system, at a BER of  $10^{-5}$ .

## KEYWORDS

BCH codes, receiver diversity, turbidity, turbulence, underwater wireless optical communication

## 1 | INTRODUCTION

Optical communication provides high data transfer rates, with no requirement for procurement of expensive bandwidth spectrum which is an essential requirement in the case of wireless communication. This advantage of optical communication has motivated researchers to devote their energies to the design and development of high-speed and reliable optical communication links. A lot of work has gone into investigating the deployment of underwater wireless optical communication (UWOC) systems for realising high-speed short-distance communication links for strategic and commercial applications. The underwater optical channel is different from the free-space optical channel. It presents higher attenuation to the propagating wave compared with the free-space channel. This is brought about by scattering and absorption of the optical signal in the water medium. Scattering deviates the path of the transmitted optical signal and absorption in the medium reduces the photon count, which in turn leads to a reduction in the intensity of received light at the receiver. A study of literature reveals that the optical wavelengths in the range of 450 to 530 nm are minimally affected by absorption and scattering.<sup>1-3</sup> In addition to absorption and scattering, beam fluctuation is one of the major limiting factors of the UWOC system. Beam fluctuations arise due to the turbulence and air bubbles present in the underwater medium.<sup>4,5</sup> In References 6 and 7, the authors have studied the analytical bit error rate (BER) performance of the on-off keying (OOK) modulated multiple-input multiple-output UWOC systems. In Reference 8, the authors mitigated the effect of underwater turbulence and improved the performance of UWOC systems using Reed-Solomon and low-density parity-check codes.

This article describes the performance of optical communication link operating through seawater with different turbidity levels contained in a tank having a volume of  $5 \times 0.5 \times 0.5 \text{ m}^3$  at a transmission speed of 1 Mbps in the presence of turbulence and air bubbles. To the best of author's knowledge in literature, researchers have addressed and mitigated only the effects of underwater turbulence using simulation and analytical methods. In this article, the

first time we have addressed the effects of underwater turbulence, air bubbles, and beam attenuation for varying turbidity levels and mitigated these effects using receiver diversity techniques and error-correcting code using experimental setup with the results being validated with analytical approach. The proposed Bose-Chaudhuri-Hocquenghem (BCH) code augmented with diversity reception combining techniques enhances the UWOC system performance in the presence of turbulence and beam attenuation.

The remaining part of this article is organized as follows, Section 2 describes the system model, Section 3 is devoted to the description of the experimental setup and statistical distribution of received irradiance, Section 4 describes the process of BCH encoding and decoding, Section 5 provides information about the analytic models used to describe lightwave propagation in seawater, Section 6 is devoted to a discussion of experimental and analytical results followed by conclusion in Section 7.

## 2 | SYSTEM MODEL

The information bits of the data source is OOK modulated with a LED source of 470 nm wavelength. Turbulence in the water medium is generated by blowing of air bubbles. At the receiver, photo-diode (PD) followed by a suitable transimpedance circuit, converts the variations in light intensity into electrical voltages. Figure 1 is a block diagram of a UWOC system employing receiver diversity combining with BCH coding, where  $L$  is the length of the underwater channel,  $s$  represents the transmitted binary data, and  $c$  is BCH encoded bit sequence, respectively. This data is input to the LED driver circuit which drives the source LED using OOK,  $D_1, D_2, \dots, D_M$  are  $M$  independent and identical PDs. A distance of 5 cm is maintained between any of two PDs in the receiver diversity combining,  $Y_1, Y_2, \dots, Y_M$  are the responses from  $D_1, D_2, \dots, D_M$ , respectively, and  $Y$  represents the response after suitable diversity combining of the outputs of the  $M$  PDs,  $\hat{c}$  and  $\hat{s}$  represents the recovered decoded data and estimated bitstreams, respectively.

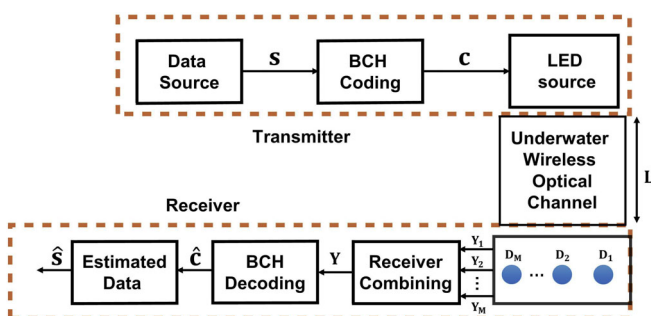


**FIGURE 1** Block diagram of receiver diversity combining UWOC [Color figure can be viewed at wileyonlinelibrary.com]

At the transmitter side, binary “1” is represented by a optical pulse of transmit power  $P_t$  and binary “0” is represented by absence of pulse (zero transmit power), respectively, for  $T_b$  sec duration. The data received at the  $i^{\text{th}}$  PD is represented by,

$$Y_i = \eta_i \sqrt{P_t T_b} \Upsilon I_i + n_i, \quad 1 \leq i \leq M \quad (1)$$

where  $\Upsilon \in \{0, 1\}$  represents the information bitstream,  $s$  for uncoded and  $c$  for BCH coded UWOC system,  $P_t$  is the transmit power of LED source,  $T_b$  is bit duration,  $I_i$ ,  $\eta_i$ , and  $n_i$  are  $i^{\text{th}}$  channel received irradiance, PD’s responsivity and additive Gaussian noise with zero mean and  $\sigma^2$  variance, respectively. Sources of noise are thermal noise, shot noise and background noise, corresponding noise source can be calculated as,<sup>9,10</sup>  $\sigma^2 = \sigma_{\text{th}}^2 + \sigma_{\text{ss}}^2 + \sigma_{\text{bg}}^2$ , where variance due to thermal noise, shot noise, and background noise are,  $\sigma_{\text{th}}^2 = 4K_b T_e B / R_L$ ,  $\sigma_{\text{ss}}^2 = 2q\eta I_d B$  and  $\sigma_{\text{bg}}^2 = 2q\eta P_{\text{BG}} B$ , respectively,  $K_b = 1.38 \times 10^{-23}$  J/K is the Boltzmann’s constant,  $T_e = 256$  is absolute receiver temperature in Kelvin,  $B = 2/T_b$  is electronic bandwidth, bit duration  $T_b = 1 \mu\text{s}$ ,  $q = 1.6 \times 10^{-19}$  C is the charge of an electron,  $\eta = 0.15$  A/W is the PD responsivity,  $I_d = 1$  nA is dark current of the PD, and  $P_{\text{BG}} = 0.1$  nW is the received background noise power.<sup>11</sup> The noise variance due to thermal, shot and background noise calculated by substituting these values in corresponding noise variance equations. From the obtained values, it is clear that the variance of thermal noise ( $\sigma_{\text{th}}^2 = 5.6 \times 10^{-16}$ ) is approximately six orders of magnitude higher than the variance of shot noise ( $\sigma_{\text{ss}}^2 = 6.4 \times 10^{-22}$ ) and approximately seven orders of magnitude greater than background noise variance ( $\sigma_{\text{bg}}^2 = 9.6 \times 10^{-24} \approx 1 \times 10^{-23}$ ). Hence thermal noise is the dominant noise source. This is modelled by the Gaussian distribution.

## 3 | EXPERIMENTAL SETUP

In this section, the major components (LED, PD, and underwater channel) involved in the UWOC system and the details of experimental setup for implementing various receiver diversity techniques are presented.

### 3.1 | LED

A blue LED of 470 nm central wavelength *LXML – PB01 – 0040* is employed to transmit optical data through the underwater medium. The maximum optical power that can be delivered by this LED source is 500 mW.<sup>12</sup>

### 3.2 | Photo-diode

Silicon PD *FDS 100* is employed at the receiver to detect the transmitted optical data. Figure 2 shows the receiver circuit diagram. The power supply voltage undergoes low pass filtering prior to being applied to the PD.<sup>11</sup> This low pass

filter is constructed using the resistor-capacitor pair,  $R_1$ ,  $C_1$ . It is used to protect the PD from the sudden changes in the bias voltage. The response of PD is given to load resistance ( $R_L$ ), which converts incident optical energy into equivalent voltage levels (data reconstruction). We have chosen  $R_1$  equal to 1 K $\Omega$ ,  $C_1$  equal to 0.1  $\mu$ F, which yields a low pass filter cut-off frequency of 1.6 kHz, the bias voltage is chosen to be 15 V, and load resistance  $R_L = 50 \Omega$ .

### 3.3 | Underwater channel

Seawater is a mixture of water with various chemical elements and materials, which can induce refractive index variation in the channel. This can cause attenuation (absorption and scattering) of the propagating optical

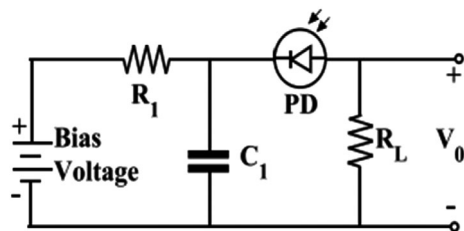


FIGURE 2 Receiver circuit diagram

beam, which affects the performance of the UWOC system. The substances commonly found in seawater are chlorophyll, dissolved organic and inorganic materials and sediment. As a result of the presence of these materials, the medium exhibits turbidity. The measured values of conductivity, salinity, turbidity, absorption, and scattering for a seawater sample collected from the Arabian sea (near NITK Surathkal) have been tabulated in Table 1. Figure 3 shows the experimental results of the absorption of light for different wavelength light sources. It is evident that absorption is minimum at 470 to 530 nm (blue, green) and 620 to 700 nm (red) wavelengths. This result has been obtained with the help of the AU 2701 model UV-VIS double beam spectrophotometer.

In addition to attenuation brought about by absorption and scattering, underwater turbulence has the potential to degrade the performance of the UWOC system further. In our setup, we have made arrangements to create an environment to study the effects of these phenomena. To induce turbulence in a turbid environment, four aerating jets (each having an airflow rate of 3 l/m) are used to generate different sized bubbles. Two wavemakers (an airflow rate of 3.5 l/m) are used to generate waves and weak turbulence. In general, the river and seawater possess turbidity values around 5 and 10 nephelometric turbidity unit (NTU), respectively. So in this article, we have realized the UWOC

TABLE 1 Experimental measurements of seawater

Parameter	Turbidity	Conductivity	Salinity	Absorption	Scattering
Measured value	8 NTU	22.5 mS/cm	14.28 ppt	$0.095\text{m}^{-1}$	$0.3095\text{m}^{-1}$

Abbreviation: NTU, nephelometric turbidity unit.

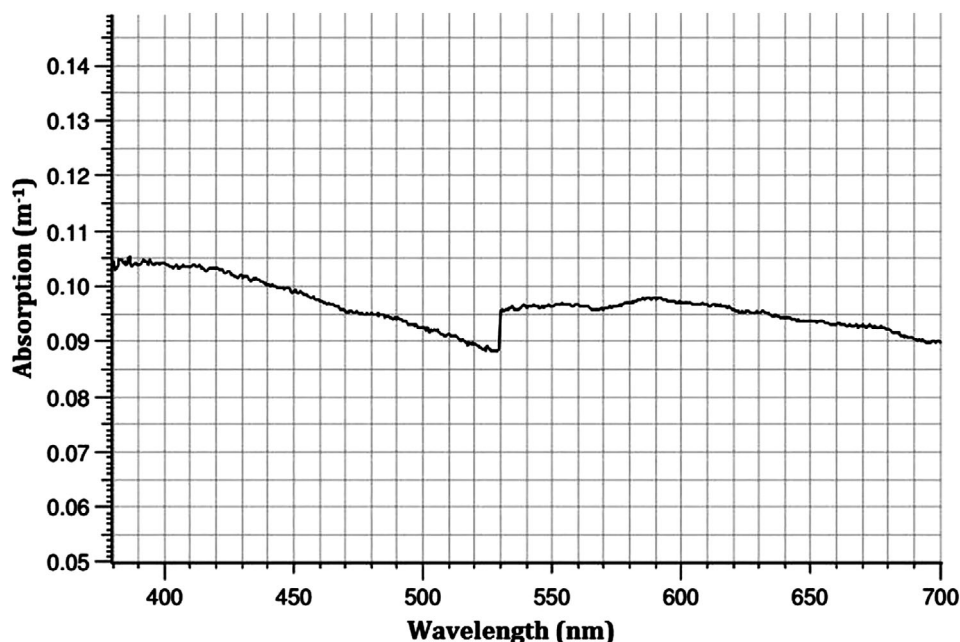
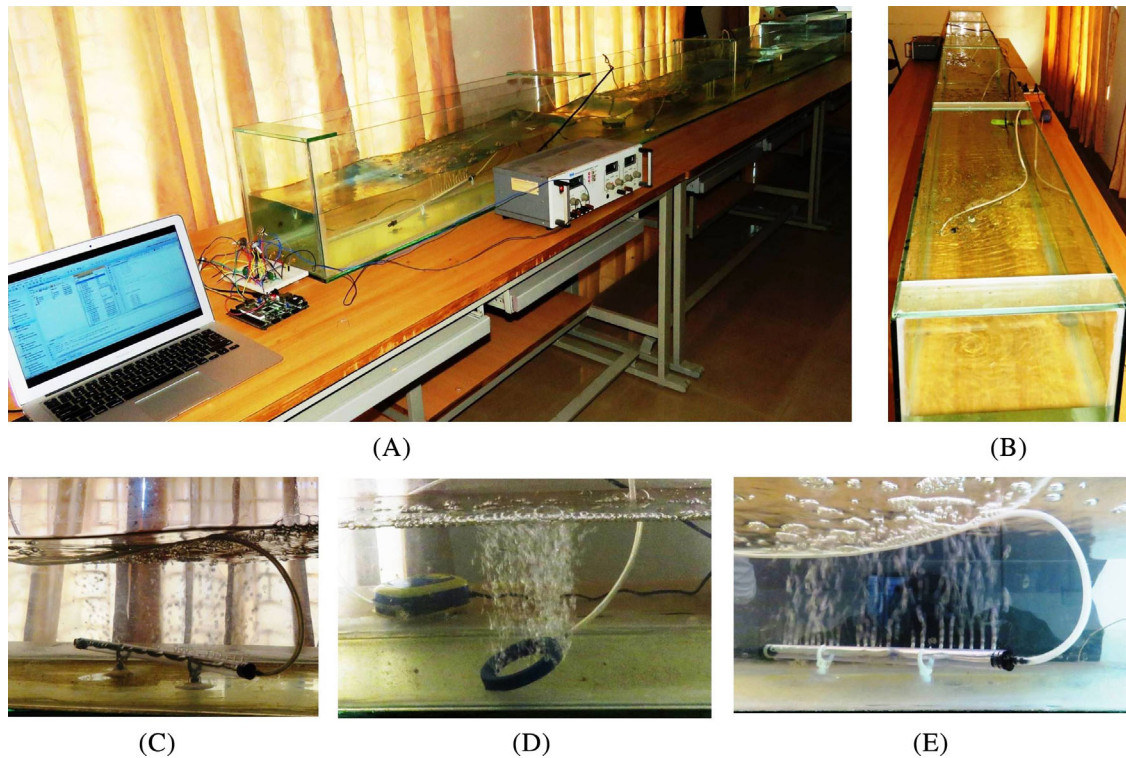
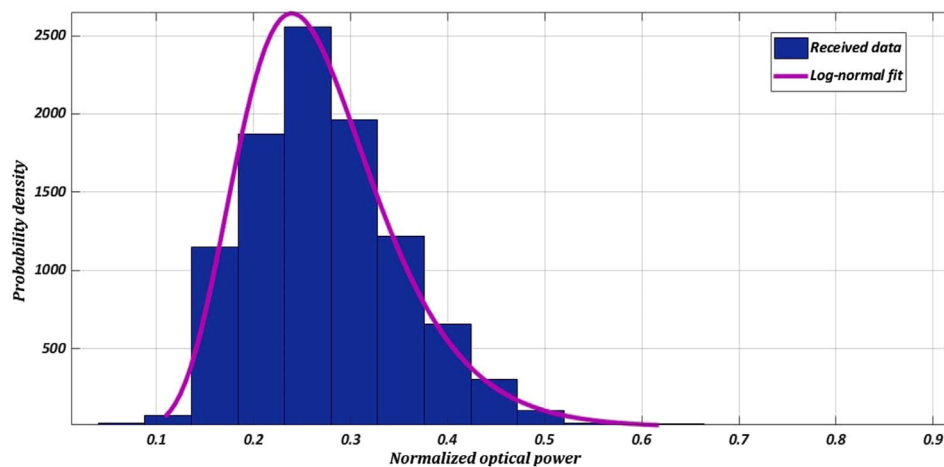


FIGURE 3 Experimental results of absorption with respect to source wavelength



**FIGURE 4** Experimental setup for the proposed UWOC system, A, front view; B, top view of 5 m link; C, Waves and weak turbulence generation using wave maker; D and E, Air bubble generation using aerating jets [Color figure can be viewed at [wileyonlinelibrary.com](http://wileyonlinelibrary.com)]



**FIGURE 5** Histogram of received data with log-normal fit [Color figure can be viewed at [wileyonlinelibrary.com](http://wileyonlinelibrary.com)]

system for 5 and 10 NTU turbidity levels. Different values of turbidity are created by the addition of calculated amounts of insoluble particles (Kaolin powder) to the water medium. Figure 4 shows the setup of the seawater channel. The effect of background noise can be minimized using an optical bandpass filter with a central wavelength of 470 nm and a band of 35 nm, which passes the information-bearing signal lying between  $(470 \pm 35)$  nm and eliminates other wavelength signals. *BP 470/35* is the optical bandpass filter we used.

### 3.4 | Channel estimation

In order to understand the behavior of the channel, a sequence of pilot bits are transmitted through the channel of length 5 m, width 0.5 m, and height 0.5 m at turbidity level of 10 NTU. The distribution of received optical power at the receiver is shown in Figure 5. It is observed that there is a good fit with the log-normal density function. Mean and variance of the received pilot data are 0.989 and  $4.8 \times 10^{-3}$ , respectively.

### 3.5 | Receiver diversity

Deploying a single LED source to  $M$  identical PDs and responses are suitably combined to enhance the UWOC system performance. The use of selection combining (SC), majority logic combining (MLC), and equal gain combining (EGC) to provide receiver diversity combining. The responses of PDs are combined as given in below.

#### 3.5.1 | Selection combining

SC selects maximum received irradiance among all the PD's response. Figure 6 shows the receiver of  $1 \times M$  SC scheme, where  $Y_1, Y_2, \dots, Y_M$  are PD responses,  $Y$  is superior (maximum) among  $Y_1, Y_2, \dots, Y_M$  and estimated data  $\hat{s}$  obtained, passing the combined response  $Y$  to a two level comparator.

#### 3.5.2 | Majority logic combining

Majority logic combining scheme recovers the transmitted data over the channel based on the majority of the logical responses of all PDs employed at the receiver. Figure 7 shows the receiver of  $1 \times M$  MLC scheme, where *mode* represents majority of incoming responses,  $Y_1, Y_2, \dots, Y_M$  are PDs response,  $\hat{s}_1, \hat{s}_2, \dots, \hat{s}_M$  are comparators responses and  $\hat{s}$  is majority of  $\hat{s}_1, \hat{s}_2, \dots, \hat{s}_M$ .

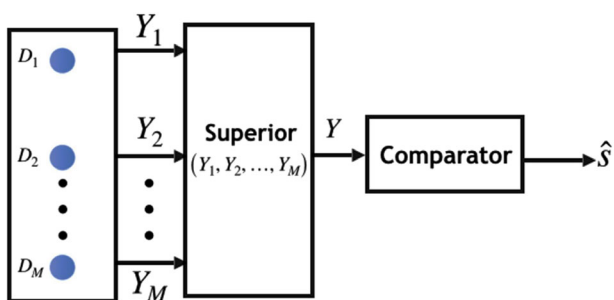


FIGURE 6  $1 \times M$  selection combining [Color figure can be viewed at wileyonlinelibrary.com]

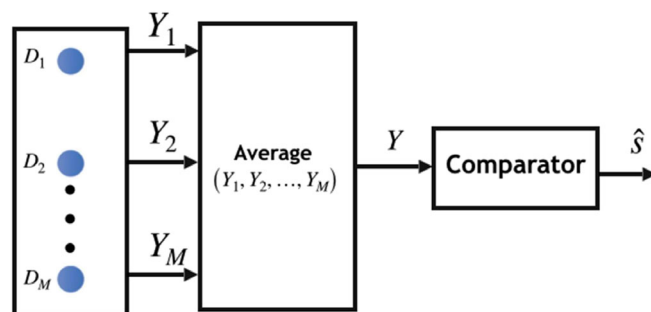


FIGURE 8  $1 \times M$  equal gain combining [Color figure can be viewed at wileyonlinelibrary.com]

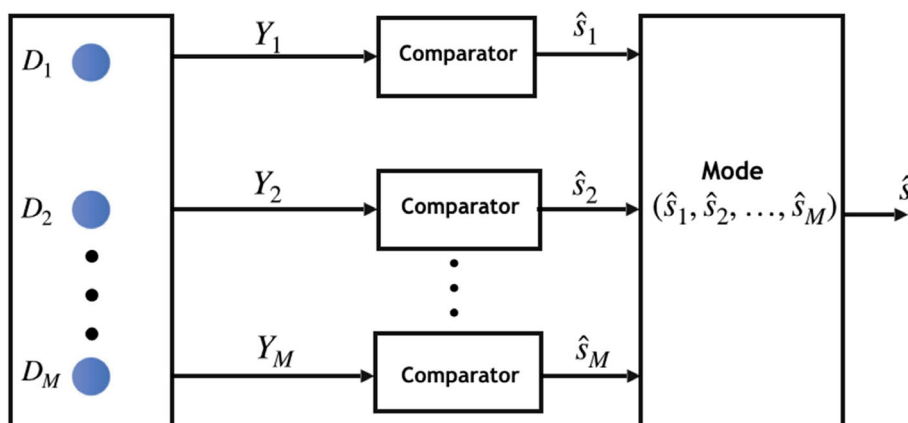


FIGURE 7  $1 \times M$  majority logic combining [Color figure can be viewed at wileyonlinelibrary.com]

#### 3.5.3 | Equal gain combining

In EGC scheme, the combined response is average of response obtained by  $M$  PDs, that is,  $Y = \sum_{i=1}^M \frac{Y_i}{M}$ . Estimated data can be obtained by passing the EGC combined data to a comparator of a suitable threshold. Figure 8 is the receiver of  $1 \times M$  EGC scheme.

## 4 | BCH CODES

In underwater channels, optical data can be attenuated (absorption and scattering) due to the presence of turbidity in the medium.<sup>13</sup> Hence, there is a finite probability that the transmitted data can be distorted and corrupted. This corruption introduces errors in the data stream. In order to detect and correct errors introduced by the medium, a suitable channel code has to be employed. Based on the experimental observation, the turbid underwater channel was adding 30% of errors in the transmitted data stream. So, we have chosen to use the  $(n = 31, k = 11)$  BCH code in this study. BCH codes are powerful  $t$  bit random error-correcting codes over the span of  $n = 2^m - 1$  bit length in the Galois field  $GF(2^m)$ , where  $m$  is any real positive integer ( $m \geq 3$ ). The field elements are represented by  $\{0, 1, \alpha, \alpha^2, \dots, \alpha^{2^m-2}\}$  (where  $\alpha$  is a

**TABLE 2** Minimal polynomial of  $GF(2^5)$  for  $t = 4$ 

Conjugacy class	Minimal polynomial
$\{\alpha, \alpha^2, \alpha^4, \alpha^8, \alpha^{16}\}$	$M_1(x) = 1 + x^2 + x^5$
$\{\alpha^3, \alpha^6, \alpha^{12}, \alpha^{24}, \alpha^{17}\}$	$M_3(x) = 1 + x^2 + x^3 + x^4 + x^5$
$\{\alpha^5, \alpha^{10}, \alpha^{20}, \alpha^9, \alpha^{18}\}$	$M_1(x) = 1 + x + x^2 + x^4 + x^5$
$\{\alpha^7, \alpha^{14}, \alpha^{28}, \alpha^{25}, \alpha^{19}\}$	$M_1(x) = 1 + x + x^2 + x^3 + x^5$

primitive element in the field  $GF(2^m)$ .<sup>14,15</sup> These elements are partitioned into conjugacy classes. Each conjugacy class has an associated minimal polynomial. The generator polynomial of a BCH code is obtained by determining the least common multiple of the minimal polynomials associated with the elements  $\alpha^b, \alpha^{b+1}, \dots, \alpha^{b+\delta-2}$ , where  $b$  is an integer  $\geq 1$  and  $\delta$  is design distance, which equals to  $2t + 1$ . The generator polynomial is computed as,

$$g(x) = \text{LCM}\{M_b(x), M_{b+1}(x), \dots, M_{b+\delta-2}(x)\} \quad (2)$$

where,  $M_i(x)$  represents the minimal polynomial of  $i^{\text{th}}$  conjugacy class. Elements in the same conjugacy class have same minimal polynomial. The generator polynomial construction for the BCH code specified by parameters,  $m = 5$ ,  $t = 4$ , and  $b = 1$  is  $g(x) = \text{LCM}\{M_1(x), M_2(x), M_3(x), M_4(x), M_5(x), M_6(x), M_7(x), M_8(x)\} = M_1(x) \times M_3(x) \times M_5(x) \times M_7(x)$ . Minimal polynomials of various conjugacy classes contained in the field  $GF(2^5)$  are provided in Table 2. The generator polynomial obtained by computing the product of minimal polynomials is,

$$g(x) = 1 + x^2 + x^4 + x^6 + x^7 + x^9 + x^{10} + x^{13} + x^{17} + x^{18} + x^{20} \quad (3)$$

Generator matrix ( $\mathbf{G}_{11 \times 31}$ ) is obtained using generator polynomial  $g(x)$ . Encoded data is obtained by carrying out the operation,  $\mathbf{c}_{1 \times 31} = \mathbf{s}_{1 \times 11} \mathbf{G}_{11 \times 31}$ . This BCH encoded data is modulated with LED and then passed through the medium. At the receiver, the data is passed through a two-level comparator with suitably designed thresholds, which are used to regenerate the data stream. This data may contain errors introduced by the channel. The Berlekamp-Massey decoding algorithm is employed to detect and correct errors in the received bitstream.<sup>16,17</sup>

## 5 | ANALYTICAL EVALUATION OF UWOC SYSTEM

In this section, we present the distribution of UWOC channel and closed-form analytical BER expressions for SISO link and  $1 \times M$  receiver diversity combining schemes with and without BCH code.

### 5.1 | Channel model

Based on the experimental results obtained in Section 3.4, the received irradiance behavior is fit with log-normal density function, so the log-normal density function is considered as a turbulence channel model for further analysis and the amount of attenuation depends on the level of turbidity in the medium. The received irradiance in the presence of attenuation and weak turbulence can be characterized as,<sup>18</sup>

$$I = I_a I_t \quad (4)$$

where,  $I_a$  is deterministic path loss constant due to the beam attenuation and is given as  $I_a = \exp(-(C(\lambda))L)$  from Beer-Lambert's law,  $C(\lambda)$  is attenuation coefficient,<sup>19</sup>  $L$  is link-range, and  $I_t$  received irradiance due to turbulence. The received irradiance due to weak underwater turbulence is modeled with log-normal density function,<sup>20</sup> which is given as,

$$f_{I_t}(I_t) = \frac{1}{2I_t} \frac{1}{\sqrt{2\pi\sigma_X^2}} \exp\left(-\frac{(\ln(I_t) - 2\mu_X)^2}{8\sigma_X^2}\right) \quad (5)$$

where,  $\mu_X$  and  $\sigma_X^2$  are mean and variance of Gaussian random variable  $X = \frac{1}{2} \ln(I_t)$ . The density function of combined turbulence and attenuation effect can be obtained as,

$$\begin{aligned} f_I(I) &= \left| \frac{d}{dI} \left( \frac{I}{I_a} \right) \right| f_{I_t} \left( \frac{I}{I_a} \right) \\ &= \frac{1}{2I} \frac{1}{\sqrt{2\pi\sigma_X^2}} \exp\left(-\frac{(\ln(I/I_a) - 2\mu_X)^2}{8\sigma_X^2}\right) \end{aligned} \quad (6)$$

From the received pilot data, the mean and variance are to be  $\mathbb{E}(I) = 0.989$  and  $\sigma_I^2 = 4.8 \times 10^{-3}$ , respectively, mathematical equations are  $\mathbb{E}(I) = \exp(2\mu_X + 2\sigma_X^2)$  and  $\sigma_I^2 = \exp(4\sigma_X^2 - 1) \times \exp(4\sigma_X^2 + 4\mu_X)$ . Equating these equations yields  $\mu_X = -6.7 \times 10^{-3}$  and  $\sigma_X^2 = 1.2 \times 10^{-3}$ .

### 5.2 | BER evaluation

In this subsection, the closed-form analytic BER expressions for SISO and  $1 \times M$  SC, MLC, and EGC combining schemes with and without BCH code have been derived.

#### 5.2.1 | Single input single output

The received OOK modulated data in the presence of turbulent underwater channel is modeled as,

$$Y = \eta I \sqrt{P_t T_b} s + n \quad (7)$$

The BER of SISO channel with equiprobable input bits (assuming known log-normal channel) is specified by,

$$P_{\text{siso}} = \frac{1}{2} \int_0^\infty \left( \sum_{i=0}^1 P \left( \frac{\hat{s} = 1 - i}{s = i, I} \right) \right) f_I(I) dI \quad (8)$$

where,  $P\left(\frac{\hat{s}=1}{s=0,I}\right)$  is the probability of estimated data being inferred as “1” when transmitted data is “0,”  $P\left(\frac{\hat{s}=0}{s=1,I}\right)$  is the probability of estimated data being inferred as “0” when transmitted data is “1” and  $f_I(I)$  is log-normal channel density function. The BER reduces to the form,

$$P_{\text{siso}} = \int_0^{\infty} \mathbb{Q}\left(r\eta I \sqrt{\frac{P_t T_b}{4\sigma^2}}\right) f_I(I) dI \quad (9)$$

where,  $r$  is code-rate, “1” for uncoded and  $k/n$  for  $(n, k)$  coded system and  $\mathbb{Q}(z) \triangleq \frac{1}{\sqrt{2\pi}} \int_z^{\infty} \exp\left(-\frac{y^2}{2}\right) dy$ . Substituting  $I$  by  $\exp(2x)$  and then evaluate Equation (9) using Gauss-Hermite quadrature polynomial as,

$$P_{\text{siso}} \approx \frac{1}{\sqrt{\pi}} \sum_{i=1}^l W_i \mathbb{Q}\left(\zeta I_a \exp\left(x_i \sqrt{8\sigma_X^2} + 2\mu_X\right)\right) \quad (10)$$

where,  $W_i$  is weight of  $i$ th order approximation and  $\zeta = r\eta \sqrt{\frac{P_t T_b}{4\sigma^2}}$ .  $P_{\text{siso}}$  is calculated for instantaneous values of  $x$ .

### 5.2.2 | Selection combining

Selection combining selects the maximum irradiance among all the irradiance of receivers. Received signal using SC is expressed as,

$$Y = \max\{Y_1, Y_2, \dots, Y_M\} = \eta \sqrt{P_t T_b} I_{sc} + n \quad (11)$$

where  $I_{sc} = \max(I_1 I_a, I_2 I_a, \dots, I_M I_a)$ . The received signal is completely dependent on maximum irradiance. BER of  $M$  number of PDs SC with single-source OOK modulated is expressed as,

$$P_{sc} = \int_0^{\infty} f_{I_{sc}}(I_{sc}) \mathbb{Q}(\zeta I_{sc}) dI_{sc} \quad (12)$$

The probability density function (PDF) of SC scheme  $f_{I_{sc}}(I_{sc})$  is expressed as (refer Appendix A),

$$f_{I_{sc}}(I_{sc}) = \frac{M}{2I_{sc} \sqrt{2\pi\sigma_X^2}} \exp\left(-\frac{(\ln(I_{sc}/I_a) - 2\mu_X)^2}{8\sigma_X^2}\right) \left(\frac{1}{2} + \frac{1}{2} \operatorname{erf}\left(\frac{\ln(I_{sc}/I_a) - 2\mu_X}{\sqrt{8\sigma_X^2}}\right)\right)^{M-1} \quad (13)$$

where,  $\operatorname{erf}(x) \triangleq \frac{2}{\sqrt{\pi}} \int_0^x \exp(-t^2) dt$ . Substituting Equation (13) in Equation (12) which yields as,

$$P_{sc} = \frac{M}{\sqrt{\pi}} \int_0^{\infty} \exp(-h^2) \mathbb{Q}\left(\zeta I_a \exp\left(h \sqrt{8\sigma_X^2} + 2\mu_X\right)\right) \times \left(\frac{1}{2} + \frac{1}{2} \operatorname{erf}(h)\right)^{M-1} dh \quad (14)$$

where,  $h = (\ln(I_{sc}/I_a) - 2\mu_X) / \sqrt{8\sigma_X^2}$ . Equation (14) is computed using Gauss-Hermite quadrature polynomial as,

$$P_{sc} \approx \frac{M}{\sqrt{\pi}} \sum_{i=1}^l W_i \mathbb{Q}\left(\zeta I_a \exp\left(h_i \sqrt{8\sigma_X^2} + 2\mu_X\right)\right) \times \left(\frac{1}{2} + \frac{1}{2} \operatorname{erf}(h_i)\right)^{M-1} \quad (15)$$

where  $W_i$  and  $h_i$  are calculated for various values of  $I_{sc}$ .

### 5.2.3 | Majority logic combining

Majority logic combining scheme recovers the transmitted data over the channel based on the majority of the logical response. In this scheme, the path between the LED to an individual PD is modelled like a SISO link. Hence, the final MLC response is dependent on the responses provided by the  $M$  individual SISO links. The probability of error is evolved as,

$$P_{\text{mlc}} = \sum_{i=\lfloor \frac{M+1}{2} \rfloor}^M \binom{M}{i} P_{\text{siso}}^i (1 - P_{\text{siso}})^{M-i} \quad (16)$$

where,  $\lfloor \cdot \rfloor$  is floor operator and  $P_{\text{siso}}$  is BER of SISO obtained from Equation (10).

### 5.2.4 | Equal gain combining

The average of  $M$  identical PD's responses are combined to obtain a suitable EGC response. The combined response is  $Y = \frac{\eta \sqrt{P_t T_b} I_e}{M} + n$ , where  $I_e = I_a I_{\text{sum}}$  and  $I_{\text{sum}} = \sum_{i=0}^M I_i$ . The sum of  $M$  independent log-normal random variables having identical mean and variance is also a log-normally distributed random variable.<sup>21</sup> Hence,  $I_{\text{sum}} = \exp(2U)$  is log-normal distributed random variable, here  $U$  is Gaussian distributed random variable with mean  $\mu_U$  and variance  $\sigma_U^2$ .<sup>22</sup> The density function is given as,

$$f_{I_e}(I_e) = \frac{1}{2I_e \sqrt{2\pi\sigma_U^2}} \exp\left(-\frac{(\ln(I_e/I_a) - 2\mu_U)^2}{8\sigma_U^2}\right) \quad (17)$$

where, the Gaussian mean and variance are  $\mu_U = \frac{1}{2} \ln(M \mathbb{E}(I)) - \sigma_U^2$  and  $\sigma_U^2 = \frac{1}{4} \ln\left(1 + \frac{\exp(4\sigma_X^2) - 1}{M}\right)$ , respectively, the detailed derivation is given in Appendix B.

The BER equation of EGC with OOK modulation is obtained in a similar way of Equation (10) as,

$$P_{\text{egc}} \approx \frac{1}{\sqrt{\pi}} \sum_{i=1}^l W_i \mathbb{Q}\left(\frac{\zeta I_a}{M} \exp\left(x_i \sqrt{8\sigma_U^2} + 2\mu_U\right)\right) \quad (18)$$

### 5.2.5 | BCH code

When decoded code-word is not identical to the transmitted code-word, a decoding error is said to occur. An upper bound on the probability of decoding error  $P_d$  associated with a  $(n, k, t)$

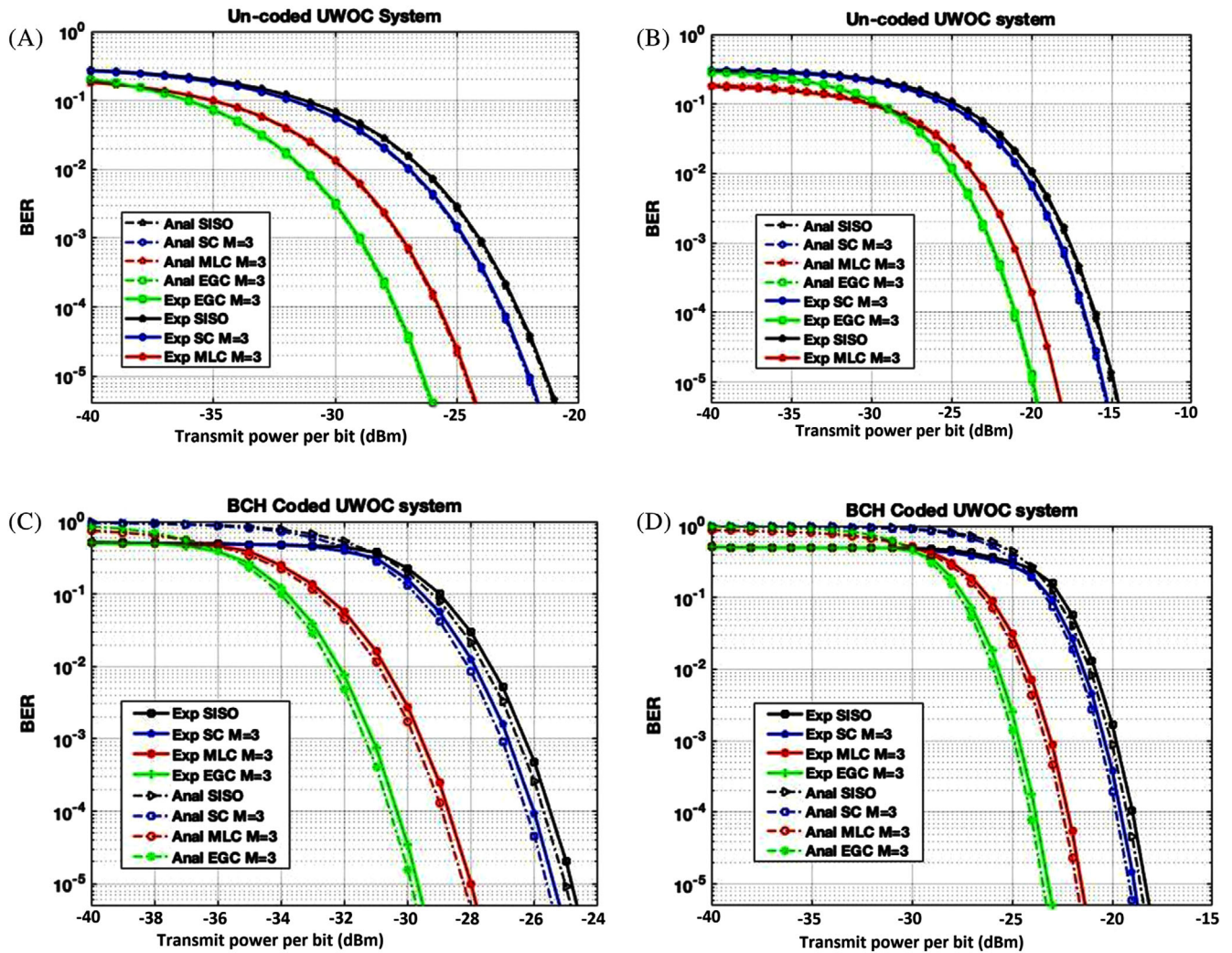


FIGURE 9  $1 \times M$  equal gain combining [Color figure can be viewed at wileyonlinelibrary.com]

nonbinary BCH code over  $GF(2^m)$  with  $t$  symbol error-correcting capability and cross over symbol error probability  $p$  is given by,<sup>16</sup>

$$P_d \leq \sum_{i=t+1}^n \binom{n}{i} p^i (1-p)^{n-i} \quad (19)$$

where  $p$  represents the binary symmetric channel transition probability. In our analysis,  $p$  corresponds to  $P_{\text{siso}}$  in Equation (10),  $P_{\text{sc}}$  in Equation (15),  $P_{\text{mlc}}$  in Equation (16) and  $P_{\text{egc}}$  in Equation (18) for SISO, SC, MLC, and EGC schemes with code-rate  $r = \frac{k}{n}$ , respectively.

## 6 | EXPERIMENTAL AND ANALYTICAL RESULTS

In the proposed UWOC system, the information bit stream at the transmitter is mapped to BCH encoding process and then OOK modulated using 470 nm blue light LED (*LXML - PB01 - 0040*). The modulated data is propagated through the turbid water which is created using insoluble particles and turbulent channel which is generated using underwater

jets and wavemakers. At the receiver side, the optical beam is detected and information stream is retrieved using multiple PD's employed with appropriate combining schemes.

In this section, we present analytical and experimental BER results with respect to transmit power for SISO,  $1 \times 3$  receiver combining (SC, MLC, and EGC) schemes with and without coding for channels having turbidity values of 5 and 10 NTU, respectively. The values of attenuation coefficients at  $\lambda = 470$  nm wavelength determined using spectrophotometer are  $C = 0.303 \text{ m}^{-1}$  for 5 NTU and  $C = 0.4505 \text{ m}^{-1}$  for 10 NTU turbidity channel.

Figure 9A,B is un-coded experimental and analytical BER results of 5 and 10 NTU turbidity level turbulent underwater channels, respectively. Figure 9A shows that a transmit power gain of more than 1 dB can be obtained by using SC, 3 dB using MLC and 5 dB using EGC over SISO at BER of  $10^{-5}$ . From Figure 9B, it can be inferred that a power gain of 0.3 dB can be obtained by using SC, 3.5 dB using MLC, and 5 dB using EGC over SISO at a BER of  $10^{-5}$ .

Figure 9C,D is ( $n = 31, k = 11$ ) BCH coded experimental and analytical BER results at 5 and 10 NTU turbidity



channels, respectively. From Figure 9C, BCH coded SC scheme can obtain 0.3 dB power gain, BCH coded MLC can obtain 2 dB power gain and BCH coded EGC can obtain 4.5 dB power gain from BCH coded SISO at BER of  $10^{-5}$ . Similarly, for 10 NTU turbidity channel more than 3 dB transmit power gain from MLC to SISO and 4 dB gain from coded EGC to coded SISO. A transmit power of at least 3 dB gain from to ( $n = 31$ ,  $k = 11$ ) BCH coded respective SISO/receiver diversity scheme. Overall from uncoded SISO to BCH coded SC, MLC, and EGC can obtain a transmit power gain of at least 4, 6, and 8 dB for 5 and 10 NTU turbidity channels, respectively.

## 7 | CONCLUSION

In this article, we have developed closed-form expressions for the BER of a UWOC system with OOK modulation in the presence of weak turbulence induced by air bubbles and beam attenuation for a 5 m link. We have compared these results with experimental data obtained by setting up an OOK modulated UWOC system with a 470 nm LED source working in an environment characterized by turbulence generated by air bubbles for a 5 m length channel. The experimental BER results in the presence of turbulence-induced air bubbles at 5 and 10 NTU turbidity levels are evaluated and plotted. We have also studied the statistical distribution of received irradiance in an underwater channel filled with seawater in the presence of turbidity and turbulence. We have demonstrated that the experimental results are well approximated by the log-normal density function. From figures, it has been shown that at least 8 dB transmit power improvement can be obtained by the use of BCH coded EGC compared with uncoded SISO for both turbidity levels.

## ORCID

Prasad Naik Ramavath  <https://orcid.org/0000-0002-9878-2295>

Prabu Krishnan  <https://orcid.org/0000-0001-9730-7997>

## REFERENCES

- [1] Smart JH. Underwater optical communications systems part 1: variability of water optical parameters. *IEEE*; 2005: 1140-1146.
- [2] Giles JW, Bankman IN. Underwater optical communications systems. Part 2: basic design considerations. *IEEE*; 2005: 1700-1705.
- [3] Kaushal H, Kaddoum G. Underwater optical wireless communication. *IEEE Access*. 2016;4:1518-1547.
- [4] Oubei HM, ElAfandy RT, Park KH, Ng TK, Alouini MS, Ooi BS. Performance evaluation of underwater wireless optical communications links in the presence of different air bubble populations. *IEEE Photon J*. 2017;9(2):1-9.
- [5] Zhao Y, Wang A, Zhu L, et al. Performance evaluation of underwater optical communications using spatial modes subjected to bubbles and obstructions. *Opt Lett*. 2017;42(22): 4699-4702.
- [6] Jamali MV, Salehi JA, Akhondi F. Performance studies of underwater wireless optical communication systems with spatial diversity: MIMO scheme. *IEEE Trans Commun*. 2016;65(3):1176-1192.
- [7] Liu W, Xu Z, Yang L. SIMO detection schemes for underwater optical wireless communication under turbulence. *Photon Res*. 2015;3(3):48-53.
- [8] Mattoussi F, Khalighi MA, Bourennane S. Improving the performance of underwater wireless optical communication links by channel coding. *Appl Optics*. 2018;57(9):2115-2120.
- [9] Jamali MV, Salehi JA. On the BER of multiple-input multiple-output underwater wireless optical communication systems. *IEEE*; 2015: 26-30.
- [10] Jaruwatanadilok S. Underwater wireless optical communication channel modeling and performance evaluation using vector radiative transfer theory. *IEEE J Select Areas Commun*. 2008;26(9): 1620-1627.
- [11] ThorLab's. FDS 100; 2017. <https://www.thorlabs.com/thorproduct.cfm?partnumber=FDS100>
- [12] LumiLED's. LXML-PB01-0040 blue LED; 2017. <https://www.lumileds.com/uploads/265/DS68-pdf>
- [13] Davies-Colley R, Smith D. Turbidity, suspended sediment, and water clarity: a review 1. *JAWRA J Am Water Res Assoc*. 2001;37 (5):1085-1101.
- [14] Lin S, Costello DJ. *Error Control Coding*. Prentice Hall: Pearson Education India; 2001.
- [15] MacWilliams FJ, Sloane NJA. *The Theory of Error-Correcting Codes*. Vol 16. Elsevier; 1977.
- [16] Blahut RE. *Algebraic Codes for Data Transmission*. Cambridge University Press; 2003.
- [17] Moon TK. *Error Correction Coding: Mathematical Methods and Algorithms*. John Wiley & Sons; 2005.
- [18] Yang F, Cheng J, Tsiftsis TA. Free-space optical communication with nonzero boresight pointing errors. *IEEE Trans Commun*. 2014;62(2):713-725.
- [19] Farid AA, Hranilovic S. Outage capacity optimization for free-space optical links with pointing errors. *J Lightwave Technol*. 2007;25(7):1702-1710.
- [20] Jamali MV, Mirani A, Parsay A, et al. Statistical studies of fading in underwater wireless optical channels in the presence of air bubble, temperature, and salinity random variations. *IEEE Trans Commun*. 2018;66(10):4706-4723.
- [21] Fenton L. The sum of log-normal probability distributions in scatter transmission systems. *IRE Trans Commun Syst*. 1960;8(1): 57-67.
- [22] Lee EJ, Chan VW. Part 1: optical communication over the clear turbulent atmospheric channel using diversity. *IEEE J Select Areas Commun*. 2004;22(9):1896-1906.
- [23] Stüber GL, Stüber GL. *Principles of Mobile Communication*. Vol 2. Norwell, MA: Kluwer; 1996.
- [24] Tsiftsis TA, Sandalidis HG, Karagiannidis GK, Uysal M. Optical wireless links with spatial diversity over strong atmospheric turbulence channels. *IEEE Trans Wirel Commun*. 2009;8(2):951-957.

[25] Mitchell RL. Permanence of the log-normal distribution. *JOSA*. 1968;58(9):1267-1272.

**How to cite this article:** Ramavath PN, Udupi SA, Krishnan P. Experimental demonstration and analysis of underwater wireless optical communication link: Design, BCH coded receiver diversity over the turbid and turbulent seawater channels. *Microw Opt Technol Lett*. 2020;1–10. <https://doi.org/10.1002/mop.32311>

#### APPENDIX A: PDF OF $I_M = \text{MAX}(I_1, I_2, \dots, I_M)$

The cumulative distribution function (CDF)  $F_{I_m}(I_m)$  for independent and identically distributed *i. i. d* channel (from Equation 6.7 of Reference 23), is

$$F_{I_m} = (F_I(I_m))^M \quad (\text{A1})$$

The PDF takes on the form (Equation 25 of Reference 24),

$$\begin{aligned} f_{I_m}(I_m) &= \frac{d}{dI_m} (F_I(I_m))^M \\ &= M(F_I(I_m))^{M-1} f_I(I_m) \end{aligned} \quad (\text{A2})$$

The log-normal CDF is  $F_I(I_m) = \frac{1}{2} + \frac{1}{2} \text{erf}\left(\frac{\ln(I_m) - 2\mu_X}{\sqrt{8\sigma_X^2}}\right)$  and PDF  $f_I(I_m)$  is described in Equation (5). Hence, the PDF of maximum of  $M$  received irradiance takes on the form

$$\begin{aligned} f_{I_m}(I_m) &= \frac{M}{2I_m \sqrt{2\pi\sigma_X^2}} \exp\left(-\frac{(\ln(I_m) - 2\mu_X)^2}{8\sigma_X^2}\right) \\ &\quad \left(\frac{1}{2} + \frac{1}{2} \text{erf}\left(\frac{\ln(I_m) - 2\mu_X}{\sqrt{8\sigma_X^2}}\right)\right)^{M-1} \end{aligned} \quad (\text{A3})$$

#### APPENDIX B: MEAN AND VARIANCE OF $U$ FOR EGC PDF

Let  $I_{\text{sum}}$  is sum of  $M$  independent identical log-normal random variables  $(I_1, I_2, \dots, I_M)$ , then  $I_{\text{sum}} = I_1 + I_2 + \dots + I_M$  is also a log-normal random variable with mean  $\mathbb{E}(I_{\text{sum}}) = M\mathbb{E}(I)$  and variance  $\sigma_{I_{\text{sum}}}^2 = M\sigma_I^2$ , here  $\sigma_I^2 = \exp(4\sigma_X^2 - 1) \times \exp(4\sigma_X^2 + 4\mu_X)$ .<sup>25</sup>  $I_{\text{sum}}$  can be represented in exponential form as,  $I_{\text{sum}} = \exp(2U)$  then  $\mathbb{E}(I_{\text{sum}}) = \exp(2\mu_U + 2\sigma_U^2)$  and  $\sigma_{I_{\text{sum}}}^2 = \exp(4\sigma_U^2 + 4\mu_U) (\exp(4\sigma_U^2) - 1)$ . Equating these equations, yields  $\sigma_U^2 = \frac{1}{4} \ln\left(\frac{\exp(4\sigma_X^2) - 1}{M} + 1\right)$  and  $\mu_U = \frac{1}{2} \ln(M\mathbb{E}(I)) - \sigma_U^2$ .